

Microstructure of the high T_c phase ($T_c \sim 111$ K) in the Sb-Pb-Bi-Sr-Ca-Cu-O system

Naoto Kijima and Ronald Gronsky

National Center for Electron Microscopy, Materials and Chemical Sciences Division, Lawrence Berkeley Laboratory, University of California, Berkeley, California 94720

Hozumi Endo and Yasuo Oguri

Research Center, Mitsubishi Kasei Corporation, 1000 Kamoshida-cho, Midori-ku, Yokohama 227, Japan

Steffen K. McKernan and Alex Zettl

Department of Physics, University of California at Berkeley and Materials and Chemical Sciences Division, Lawrence Berkeley Laboratory, Berkeley, California 94720

(Received 21 June 1990; accepted for publication 16 October 1990)

The microstructure of the high T_c phase ($T_c \sim 111$ K) in the Sb-Pb-Bi-Sr-Ca-Cu-O system has been determined using transmission electron microscopy. Its crystal structure belongs to the superspace group N_{111}^{Bbmb} , N_{111}^{Bb2b} , P_{111}^{Bbmb} or P_{111}^{Bb2b} with subcell lattice parameters $a = 5.411(1)$ Å, $b = 5.411(1)$ Å, and $c = 37.22(6)$ Å. The high T_c phase has a modulated structure with b -axis wavelengths 26.9 and 36.1 Å. Stacking faults along the c axis in the high T_c phase are much less numerous than in the Bi-Sr-Ca-Cu-O system, but comparable to the Pb-Bi-Sr-Ca-Cu-O system. Sb substitution for Ca may affect the internal strain of the crystal.

It has been reported that the substitution of Sb and/or Pb for Bi in $\text{Bi}_2\text{Sr}_2\text{Ca}_2\text{Cu}_3\text{O}_x$ increases the endpoint critical temperature ($T_{c,\text{end}}$) to 132 K.^{1,2} Hongbao *et al.* have reported that this phase is so unstable that the $T_{c,\text{end}}$ is decreased to 112 K upon forming a stable phase after thermal cycling between 77 K and room temperature.

In another manuscript,³ the superconducting properties and chemical composition of the stable high T_c phase ($T_c \sim 111$ K) in the Sb-Pb-Bi-Sr-Ca-Cu-O system were described; the Sb-bearing superconducting phase has a 4 K higher critical temperature than that in the Pb-Bi-Sr-Ca-Cu-O system. The average chemical composition of the high T_c phase is 4.3%, 2.6%, 19.2%, 21.4%, 15.8%, and 36.9% for Sb, Pb, Bi, Sr, Ca, and Cu, respectively. The summation of the Sb concentration and the Ca concentration is approximately the same for all the samples of this phase, implying that Sb substitutes for Ca, and oxygen atoms are introduced to compensate the oxygen deficiency in the central Cu-O layer sandwiched by the two Ca layers in the crystal structure of the high T_c phase. In order to further clarify the role of the Sb atoms in the high T_c phase, this detailed study of its microstructure has been undertaken.

A sample with nominal composition $\text{Sb}_{0.10}\text{Pb}_{0.50}\text{Bi}_{1.40}\text{Sr}_{2.00}\text{Ca}_{2.00}\text{Cu}_{3.00}\text{O}_x$ was prepared by a solid-state reaction in air as described in another report.³ X-ray powder diffraction measurements were carried out using a Siemens D500 diffractometer with Cu $K\alpha$ radiation. Electrical resistivity was measured by the standard dc four-terminal method. Magnetic susceptibility was measured using a S.H.E. SQUID magnetometer in a magnetic field of 20 G. Transmission electron microscopy was carried out using a JEM-200CX high-resolution electron microscope and a JEM-200CX analytical electron microscope, both operated at 200 kV. All specimens for electron microscopy were prepared by ion milling.

Figure 1 shows the temperature dependence of the

electrical resistivity and the magnetic susceptibility of the material. The $T_{c,\text{end}}$ and $T_{c,\text{mid}}$ of the sample are 110 and 112 K, respectively, while the critical temperature for the onset of diamagnetism is 111 K. The sample therefore has a 4–5 K higher critical temperature than the high T_c phase in the Pb-Bi-Sr-Ca-Cu-O system. The data also show that the sample contains only the high T_c phase ($T_c \sim 111$ K) and none of the lower T_c phase ($T_c \sim 80$ K) of the Sb-Pb-Bi-Sr-Ca-Cu-O system.

Figure 2 shows four different zone axis electron diffraction patterns of the high T_c phase in the Sb-Pb-Bi-Sr-Ca-Cu-O system. Primary reflections with indices hkl ($h+l=2n+1$), $0kl$ ($k=2n+1$, $l=2n+1$), and $hk0$ ($h=2n+1$, $k=2n+1$) show extinctions, indicating that the space group of the average crystal structure of the high T_c phase is $Bbmb$ or $Bb2b$, the same as that of the high T_c phase ($T_c \sim 107$ K) in the Pb-Bi-Sr-Ca-Cu-O system.⁴ Although Matsui *et al.*⁵ have reported that the high T_c phase ($T_c \sim 107$ K) in the Bi-Sr-Ca-Cu-O system has an ideal body-centered orthorhombic structure, a more accurate description is that this crystal structure belongs to either the $Bbmb$ or $Bb2b$ space groups because of the appearance of reflections with hkl indices satisfying ($h+l=2n$) in its

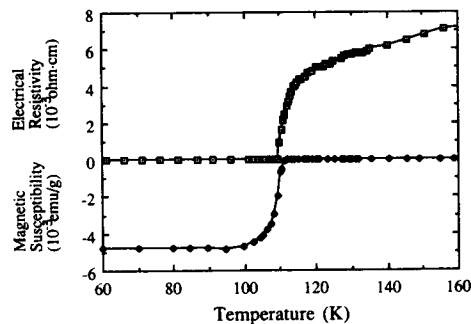


FIG. 1. Temperature dependence of the electrical resistivity and the magnetic susceptibility of the superconductor in the Sb-Pb-Bi-Sr-Ca-Cu-O system. The $T_{c,\text{end}}$ and $T_{c,\text{mid}}$ of the sample are 110 and 112 K, respectively. The critical temperature for the onset of diamagnetism is 111 K.

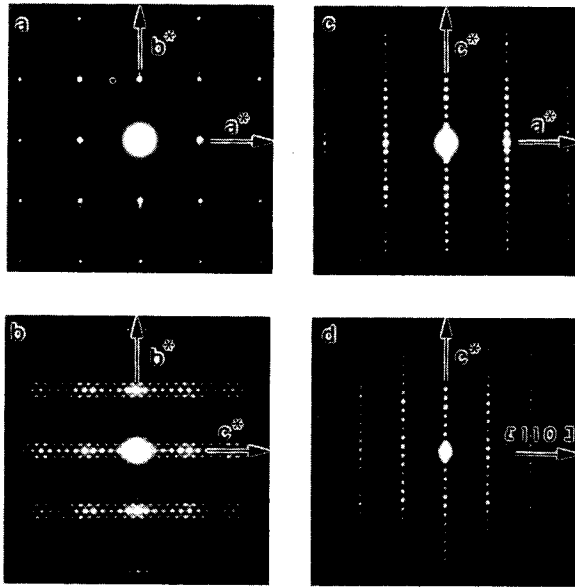


FIG. 2. Selected area diffraction patterns of the high T_c phase in the Sb-Pb-Bi-Sr-Ca-Cu-O system. (a) a^*-b^* plane, (b) b^*-c^* plane, (c) a^*-c^* plane, (d) $(a^* + b^*)-c^*$ plane. The superspace group of the high T_c phase is N_{111}^{Bbmb} , N_{111}^{Bb2b} , P_{111}^{Bbmb} , or P_{111}^{Bb2b} .

diffraction patterns. The space group of the average crystal structure of the high T_c phase ($T_c \sim 111$ K) in the Sb-Pb-Bi-Sr-Ca-Cu-O system is the same as the high T_c phase ($T_c \sim 107$ K) in both the Pb-Bi-Sr-Ca-Cu-O and Bi-Sr-Ca-Cu-O systems.

Satellite spots are clearly observed in the diffraction patterns of the a^*-b^* and b^*-c^* reciprocal planes. Figure 3 shows a magnified version of the electron diffraction pattern in Fig. 2(b) and the corresponding phase contrast image. Two types of satellite spots are observed in the electron diffraction pattern. One set of satellites is oblique to the b^* axis, and is marked (A). The b -axis component of the corresponding modulation has a wavelength of 26.9 Å. The other set of satellites occurs along the b^* axis with a wavelength of 36.1 Å, and is marked (B). The former modulated structure is the same as those observed in both the Bi-Sr-Ca-Cu-O system and Pb-Bi-Sr-Ca-Cu-O system, while the latter is closer to the one observed only in the Pb-Bi-Sr-Ca-Cu-O system. Many reports have been published on the modulated structure in the high T_c phase of the Pb-Bi-Sr-Ca-Cu-O system, citing wavelengths of 27 and 45–54 Å along the b^* axis.^{6–8} It is noted for comparison that although the direction of the modulation with the wavelength of 45–54 Å in the Pb-Bi-Sr-Ca-Cu-O system is the same as the one (marked “B”) in the Sb-Pb-Bi-Sr-Ca-Cu-O system, the wavelength is substantially smaller for the Sb-bearing material.

Assigning four indices H , K , L , and m to both primary and satellite reflections in accordance with the procedure described by de Wolff *et al.*⁹ we find that the allowed satellites marked (A) have indices $HKLm$ ($H + L + m = 2n$), $HK0m$ ($K = 2n$), and $0KLM$ ($K = 2n$) where $H = h$, $K = k$, $L = l + m$. This corresponds to the superspace group N_{111}^{Bbmb} or N_{111}^{Bb2b} , which is the same as that of the modulated structure observed in both the Bi-Sr-Ca-Cu-O system and Pb-Bi-Sr-Ca-Cu-O system. However, the

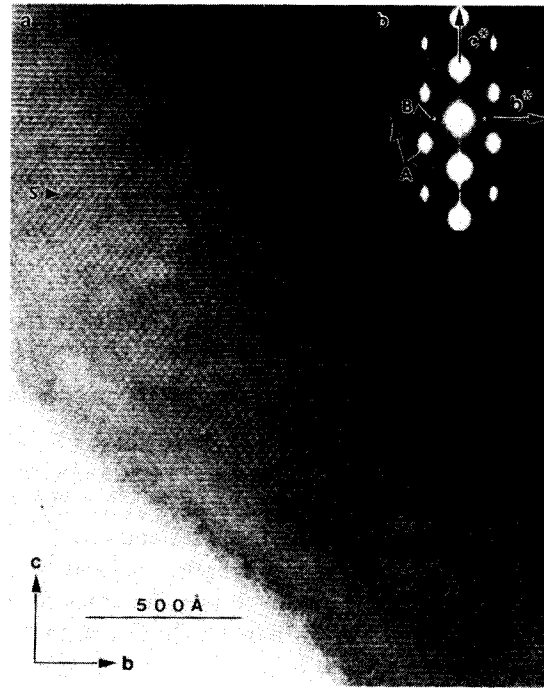


FIG. 3. (a) Phase contrast high-resolution transmission electron microscope image and (b) corresponding selected area diffraction pattern of the high T_c phase in the Sb-Pb-Bi-Sr-Ca-Cu-O system with the incident beam along the a axis. Note that there are two types of satellite spots marked (A) and (B) in the diffraction pattern. The b -axis components of wave vectors of modulated structures corresponding to the satellite spots (A) and (B) have magnitudes of 26.9 and 36.1 Å, respectively. The modulated structure with a wavelength of 26.9 Å is observed in the image. Note also that only one c -plane stacking fault is apparent in the image and is marked (s).

allowed satellites marked (B) have indices $HKLm$ ($H + L = 2n$), $HK0m$ ($K = 2n$), and $0KLM$ ($K = 2n$), where $H = h$, $K = k$, and $L = l$. This corresponds to the superspace group P_{111}^{Bbmb} or P_{111}^{Bb2b} , which is the same as that of the modulated structure observed only in the Pb-Bi-Sr-Ca-Cu-O system.

Lattice parameters of the average crystal structure of the high T_c phase ($T_c \sim 111$ K) in the Sb-Pb-Bi-Sr-Ca-Cu-O system were determined by x-ray powder diffraction coupled with electron diffraction. The lattice parameters are $a = 5.411(1)$ Å, $b = 5.411(1)$ Å, and $c = 37.22(6)$ Å, and are close to those of the high T_c phase ($T_c \sim 107$ K) in the Pb-Bi-Sr-Ca-Cu-O system.⁴ Although Sb^{3+} has a smaller ionic radius than Ca^{2+} , Sb substitution for about 20% of the Ca sites³ does not cause significant shrinkage of the lattice parameter in the c -axis direction.

A stacking fault along the c axis is observed in the high-resolution electron micrograph [marked “s” in Fig. 3(a)]. It was found that the density of stacking faults in this crystal is much less than that in the Bi-Sr-Ca-Cu-O system but roughly the same as that in the Pb-Bi-Sr-Ca-Cu-O system. Previous studies suggest that Pb acts as a fluxing agent in the Bi-Sr-Ca-Cu-O system that decreases the density of the stacking faults and increases crystal size.^{10–12} Given that Sb_2O_3 , like PbO , is also a low melting point compound, it could be that Sb also acts as a fluxing agent, assisting the solid-state reaction that forms the high

TABLE I. Summary of the microstructures of the Bi-based high T_c phases.

| System | T_c (K) | Superspace group | a | Subcell lattice parameters (Å) | | | Wavelength of modulated structure (Å) | Stacking faults |
|-------------------------------|-----------|--|----------|--------------------------------|-----------|-------|---------------------------------------|-----------------|
| | | | | b | c | | | |
| Bi-Sr-Ca-Cu-O ^{a,b} | 107 | $N_{\bar{1}\bar{1}\bar{1}}^{Bbmb}$ or N_{111}^{Bb2b} | 5.4 | 5.4 | 36.8 | 27 | many | |
| Pb-Bi-Sr-Ca-Cu-O ^c | 107 | $N_{\bar{1}\bar{1}\bar{1}}^{Bbmb}$ or N_{111}^{Bb2b} | 5.407(6) | 5.407(6) | 37.051(7) | 27 | few | |
| | | $P_{\bar{1}\bar{1}\bar{1}}^{Bbmb}$ or P_{111}^{Bb2b} | | | | 45–54 | | |
| Sb-Pb-Bi-Sr-Ca-Cu-O | 111 | $N_{\bar{1}\bar{1}\bar{1}}^{Bbmb}$ or N_{111}^{Bb2b} | 5.411(1) | 5.411(1) | 37.22(6) | 26.9 | few | |
| | | $P_{\bar{1}\bar{1}\bar{1}}^{Bbmb}$ or P_{111}^{Bb2b} | | | | 36.1 | | |

^aReference 5.

^bN. Kijima, H. Endo, J. Tsuchiya, A. Sumiyama, M. Mizuno, and Y. Oguri, Jpn. J. Appl. Phys. **27**, L821 (1988).

^cReferences 4, 6–8.

T_c phase in the Sb-Pb-Bi-Sr-Ca-Cu-O system with reduced stacking fault formation.

Table I shows a summary of the microstructures of the high T_c phases in the Bi-Sr-Ca-Cu-O system, the Pb-Bi-Sr-Ca-Cu-O system, and the Sb-Pb-Bi-Sr-Ca-Cu-O system. The high T_c phase ($T_c \sim 111$ K) in the Sb-Pb-Bi-Sr-Ca-Cu-O system has two types of structural modulations with wavelengths of 26.9 and 36.1 Å, similar to those of the high T_c phase in the Pb-Bi-Sr-Ca-Cu-O system. The high T_c phase ($T_c \sim 111$ K) has a small number of stacking faults along the c axis, equal in number to those in the high T_c phase of the Pb-Bi-Sr-Ca-Cu-O system and much less than those in the high T_c phase of the Bi-Sr-Ca-Cu-O system. These results suggest that Sb not only acts as a flux in the solid-state reaction but also substitutes directly into the lattice of the high T_c phase ($T_c \sim 111$ K) in the Sb-Pb-Bi-Sr-Ca-Cu-O system, forming the characteristic modulated structures and a small number of stacking faults along the c axis. As we mentioned in another report,³ the chemical composition of the high T_c phase in the Sb-Pb-Bi-Sr-Ca-Cu-O system implies that Sb substitutes for Ca, and that oxygen atoms are introduced to compensate the resulting oxygen deficiency in the central Cu-O layer sandwiched by the two Ca layers in the crystal structure. Since the ionic radius of Sb^{3+} is much smaller than that of Ca^{2+} , Sb substitution for Ca may actually affect the internal strain of the crystal.

In conclusion, the microstructure of the high T_c phase ($T_c \sim 111$ K) in the Sb-Pb-Bi-Sr-Ca-Cu-O system has been determined using transmission electron microscopy. The crystal structure of the high T_c phase has been found to belong to the superspace group $N_{\bar{1}\bar{1}\bar{1}}^{Bbmb}$, N_{111}^{Bb2b} , $P_{\bar{1}\bar{1}\bar{1}}^{Bbmb}$, or P_{111}^{Bb2b} with subcell lattice parameters $a = 5.411(1)$ Å, $b = 5.411(1)$ Å, and $c = 37.22(6)$ Å, which is very similar to the high T_c phases in the Bi-Sr-Ca-Cu-O and Pb-Bi-Sr-Ca-Cu-O systems. The high T_c phase ($T_c \sim 111$ K) has structural modulations with wavelengths of 26.9 and 36.1 Å. The former modulated structure is the same as those

observed in the high T_c phases of both the Bi-Sr-Ca-Cu-O system and Pb-Bi-Sr-Ca-Cu-O system, while the latter one is closer (but much smaller) than that observed only in the high T_c phase of the Pb-Bi-Sr-Ca-Cu-O system. A few stacking faults along the c axis are observed in the high T_c phase in the Sb-Pb-Bi-Sr-Ca-Cu-O system; however, the density of the stacking faults is much smaller than that of the high T_c phase in the Bi-Sr-Ca-Cu-O system. Sb substitution for Ca in the superconducting crystal appears to affect the internal strain of the crystal, forming both the characteristic modulated structures and a small number of stacking faults along the c axis.

This work was supported by the Director, Office of Energy Research, Office of Basic Energy Sciences, Materials Sciences Division, of the U.S. Department of Energy under contract No. DE-AC03-76SF00098.

¹L. Hongbao, C. Liezhao, Z. Ling, M. Zhigiang, L. Xiaoxian, Y. Zhi-dong, X. Bai, M. Xianglei, Z. Guen, R. Yaozhong, C. Zhaojia, and Z. Yuheng, Solid State Commun. **69**, 867 (1989).

²M. R. Chandrachood, I. S. Mulla, and A. P. B. Sinha, Appl. Phys. Lett. **55**, 1472 (1989).

³N. Kijima, R. Gronsky, H. Endo, Y. Oguri, S. K. McKernan, and A. Zettl, Jpn. J. Appl. Phys. (to be published).

⁴N. Kijima, H. Endo, J. Tsuchiya, A. Sumiyama, M. Mizuno, and Y. Oguri, Jpn. J. Appl. Phys. **28**, L787 (1989).

⁵Y. Matsui, S. Takekawa, H. Nozaki, A. Umezono, E. Takayama Muro-machi, and S. Horiuchi, Jpn. J. Appl. Phys. **27**, L1241 (1988).

⁶R. Ramesh, B. van Tendeloo, G. Thomas, S. M. Green, and H. L. Luo, Appl. Phys. Lett. **53**, 2220 (1988).

⁷S. Ikeda, K. Aota, T. Hatano, and K. Ogawa, Jpn. J. Appl. Phys. **27**, L2040 (1988).

⁸Y. Ikeda, M. Takano, Z. Hiroi, K. Oda, H. Kitaguchi, J. Takada, Y. Miura, Y. Takeda, O. Yamamoto, and H. Mazaki, Jpn. J. Appl. Phys. **27**, L2067 (1988).

⁹P. M. de Wolff, T. Janssen, and A. Janner, Acta Cryst. A **37**, 625 (1981).

¹⁰R. Ramesh, G. Thomas, S. Green, C. Jiang, Y. Mei, M. L. Rudee, and H. L. Luo, Phys. Rev. B **38**, 7070 (1988).

¹¹M. Mizuno, H. Endo, J. Tsuchiya, N. Kijima, A. Sumiyama, and Y. Oguri, Jpn. J. Appl. Phys. **27**, L1225 (1988).

¹²T. Hatano, K. Aota, S. Ikeda, K. Nakamura, and K. Ogawa, Jpn. J. Appl. Phys. **27**, L2055 (1988).